



Research paper

Correlation between catalysis and tertiary structure arrangement in an archaeal halophilic subtilase

Tatiana A.C.B. Souza^{a,1}, Débora N. Okamoto^{b,1}, Diego M. Ruiz^c, Lilian C.G. Oliveira^b, Márcia Y. Kondo^b, Ivarne L.S. Tersario^d, Luiz Juliano^b, Rosana E. De Castro^c, Iuri E. Gouvea^{b,**}, Mário T. Murakami^{a,*}

^a Laboratório Nacional de Biotecnologia, Centro Nacional de Pesquisas em Energia e Materiais, Giuseppe Maximo Scalfaro, 10000, Campinas 13083-970, Brazil

^b Departamento de Biofísica, Universidade Federal de São Paulo, Rua Três de Maio, 100, São Paulo, Brazil

^c Instituto de Investigaciones Biológicas, Facultad de Ciencias Exactas y Naturales, Universidad Nacional de Mar del Plata, Mar del Plata, Argentina

^d Centro Interdisciplinar de Investigación Bioquímica, Universidade de Mogi das Cruzes, SP, Brazil

ARTICLE INFO

Article history:

Received 6 May 2011

Accepted 21 November 2011

Available online 8 December 2011

Keywords:

Natrialba magadii
Extracellular protease
Halophilism
Structure
Stability
Kinetics

ABSTRACT

Nep (*Natrialba magadii* extracellular protease) is a halolysin-like peptidase secreted by the halophilic archaeon *N. magadii* that exhibits optimal activity and stability in salt-saturated solutions. In this work, the effect of salt on the function and structure of Nep was investigated. In absence of salt, Nep became unfolded and aggregated, leading to the loss of activity. The enzyme did not recover its structural and functional properties even after restoring the ideal conditions for catalysis. At salt concentrations higher than 1 M (NaCl), Nep behaved as monomers *in solution* and its enzymatic activity displayed a nonlinear concave-up dependence with salt concentration resulting in a 20-fold activation at 4 M NaCl. Although transition from a high to a low-saline environment (3–1 M NaCl) did not affect its secondary structure contents, it diminished the enzyme stability and provoked large structural rearrangements, changing from an elongated shape at 3 M NaCl to a compact conformational state at 1 M NaCl. The thermodynamic analysis of peptide hydrolysis by Nep suggests a significant enzyme reorganization depending on the environmental salinity, which supports *in solution* SAXS and DLS studies. Moreover, solvent kinetic isotopic effect (SKIE) data indicates the general acid-base mechanism as the rate-limiting step for Nep catalysis, like classical serine-peptidases. All these data correlate the Nep conformational states with the enzymatic behavior providing a further understanding on the stability and structural determinants for the functioning of halolysins under different salinities.

© 2011 Elsevier Masson SAS. All rights reserved.

1. Introduction

The superfamily of subtilisin-like serine peptidases (subtilases), widespread in both prokaryotic and eukaryotic organisms, constitutes a heterogeneous group of enzymes ranging from degradative to highly specific processing activities that underlies great attention from both basic and applied sciences community [1].

Subtilases display a number of biotechnological applications and a larger scope of their use can be projected based on improved and expanded properties [2,3]. Several studies have been focused on increasing or changing the substrate specificity and the catalytic properties of subtilisins [4–8]. The search for distinct subtilases members has led substantial efforts, particularly on enzymes isolated from extremophiles [9–12]. A considerable number of halophilic (from Greek *hals* = salt, *phil* = affinity) subtilases have been isolated from archaea and bacteria adapted to live in hypersaline environments [13–19]. Although these kingdoms possess different strategies to cope with the extreme osmotic pressure [20,21], secreted subtilases are directly exposed to environmental salt composition. Thus, these peptidases are instrumental tools for understanding the mechanisms involved in protein adaptation to function under extreme conditions.

Both archaeal and bacterial halophilic subtilases show maximal activity and stability in the presence of 3–4 M NaCl (reviewed in [14]). By primary sequence homology, it was demonstrated that

Abbreviations: Nep, *Natrialba magadii* extracellular protease; DMSO, dimethyl sulfoxide; MCA, 7-amino-4-trifluoromethyl coumarin; SKIEs, solvent kinetic isotope effects; CD, circular dichroism; DLS, dynamic light scattering; SAXS, small angle X-ray scattering.

* Corresponding author. Tel.: +55 19 3512 1106; fax: +55 19 3512 1100.

** Corresponding author. Fax: +55 11 5575 9617.

E-mail addresses: iuri.gouvea@unifesp.br (I.E. Gouvea), mario.murakami@lnbio.org.br (M.T. Murakami).

¹ Both authors have contributed equally to this work.

both groups exhibit an excess of negatively charged residues on their surface, which has been addressed to their halophilism. While mature bacterial subtilases are composed only by a subtilisin-like catalytic domain, the halophilic archaeal subtilases (halolysins) cloned and characterized so far (GB:285299 – [22], GB:1536794 – [23], GB:119951970 – [24], GB:AY800382 – [15]) possess an additional C-terminal domain consisting of approximately 120 amino-acids residues. Removal of this tail region abolished proteinase activity in halolysin R4 produced by *Haloferax mediterranei* [23], indicating that it provides an essential (but so far unknown) function in halolysins.

In order to gain insight into the molecular basis of activity and conformational stability of halolysins under different salt concentration, we used the secreted subtilase produced by the haloalkaliphilic archaeon *Natrialba magadii*¹(Nep) as a protein model. Nep was purified and characterized from *N. magadii* stationary phase cultures [25] and overproduced as an active enzyme in *Haloferax volcanii* cells [25]. In this work, the enzymatic activity, stability and *in solution* structural behavior of Nep were characterized under different stressful conditions. Our results correlate catalytic activity of Nep with its stability, monodispersivity and conformational changes, providing a clear notion of the structural requirements for its proper functioning under hypersaline environments.

2. Materials and methods

2.1. Materials

Anhydrous dimethyl sulfoxide (DMSO), heavy water with 99.9% (w/w) deuterium content and anhydrous methanol were purchased from Sigma–Aldrich (St Louis, MO, USA). All buffer salts were purchased from Fisher Scientific (Pittsburgh, PA, USA) or Sigma–Aldrich (St Louis, MO). Suc-Ala-Ala-Pro-Phe-MCA was provided by the Peptide Institute Inc. (Osaka, Japan).

2.2. Enzyme production and purification

Recombinant *N. magadii* ATCC 43099 extracellular protease (Nep) was expressed in *H. volcanii* DS70 as previously described [24]. Briefly, the *H. volcanii* cells harboring the Nep coding region cloned into the shuttle plasmid vector pJAM202 were grown to stationary phase (OD₆₀₀ of 1.8–2.5) in YPC medium supplemented with 2 µg novobiocin per mL. Cell-free culture medium containing Nep was concentrated and subjected to size-exclusion chromatography using a Superdex S-200 column and the buffer 50 mM Tris–HCl (pH 8.0) with 3 M NaCl as mobile phase [24]. Nep production and purification were analyzed by SDS PAGE (10%) and peptidase activity using Suc-Ala-Ala-Pro-Phe-MCA as substrate.

2.3. Kinetic determination of Nep hydrolytic activity

The hydrolysis of Suc-Ala-Ala-Pro-Phe-MCA by Nep (0.23 µM) was quantified by measuring the fluorescence at 460 nm (excitation wavelength of 380 nm) in a Hitachi F-2500 spectrofluorimeter. The concentration of dimethyl sulfoxide (DMSO) in assay buffers was kept below 1% (v/v). The reaction rate was converted into micromoles of substrate hydrolyzed per minute based on a calibration curve obtained from the complete hydrolysis of the peptide. The data were fitted with their respective standard errors to the Michaelis–Menten equation using GraFit software (Erithacus Software Limited). All experiments were performed in triplicate and the error values were less than 10% for each of the obtained kinetic parameters.

2.4. The pH dependence of Nep hydrolytic activity

The pH dependence of Suc-Ala-Ala-Pro-Phe-MCA hydrolysis was followed under pseudo-first-order rate constants at 37 °C in a four-component buffer comprised of 25 mM acetic acid, 25 mM MES, 75 mM Tris and 25 mM glycine and 1 mM EDTA (standard buffer), adjusted to the required pH by addition of 1 M NaOH or 1 M HCl. The data were fitted with the GraFit software to the appropriate equation.

2.5. Salt effect on Nep activity and stability

The effect of NaCl on the catalytic activity of Nep was investigated over a concentration range of 0.5–4 M. The assays were performed measuring the initial velocity of hydrolysis of 20 µM Suc-Ala-Ala-Pro-Phe-MCA as substrate, at 37 °C in 50 mM Tris–HCl (pH 8.0). The effect of NaCl on Nep stability was analyzed by measuring remaining activity after incubation with 0–4 M NaCl for up to 15 days under the same conditions described above.

2.6. Temperature effect on Nep stability

The effect of temperature on Nep stability was analyzed over the temperature ranging from 37 to 65 °C in 50 mM Tris–HCl (pH 8.0) buffer containing 1, 2 or 3 M NaCl. Enzyme samples (12 µg/mL) were incubated at the desired temperatures using a peltier system in a PCR Thermocycler (BIORAD). The remaining activity was measured at 37 °C under the same conditions described above.

2.7. Determination of inactivation rate constant

Thermal inactivation kinetics of the purified protease was determined by first-order expression:

$$dE/dt = -k_{\text{inat}}E$$

So that

$$\ln[E_t/E_0] = -k_{\text{inat}}t \quad (1)$$

The k_{inat} (inactivation rate constant or first-order rate constant) values were calculated from slopes obtained in $\ln[E_t/E_0]$ or $\ln[\text{residual activity}]$ versus t (time) plot at a particular temperature. The apparent half-lives were estimated by the equation:

$$t_{1/2} = \ln(2)/k_{\text{inat}}$$

The half-life is the time at which the residual activity reaches 50%.

2.8. Temperature dependence of the specificity and inactivation rate constants

Temperature dependence of the specificity constant (k_{cat}/K_M) was determined as earlier described [26,27]. The hydrolysis of Suc-AAPF-MCA by Nep was monitored under pseudo-first-order conditions ($[S] \ll K_M$) in Tris–HCl pH 8.0 buffer in the presence of 1, 2 or 3 M NaCl. Temperature corrections were applied to Tris buffer according to the equation $\Delta pK_a/\Delta t = -0.027$. Activation parameters were calculated from the linear plot of $\ln[(k_{\text{cat}}/K_M)/T]$ versus $1/T$ (Eyring Plot, Eq. (2))

$$\ln[(k_{\text{cat}}/K_M)T] = \ln(R/N_A h) + \Delta S^*/R - \Delta H^*/RT \quad (2)$$

where R is the gas constant (8.314 J mol^{−1} K^{−1}), T is the absolute temperature, N_A is the Avogadro number, h is the Plank constant, $\Delta H^* = -(\text{slope}) \times 8.314 \text{ J mol}^{-1}$ is the enthalpy of activation and

$\Delta S^* = (\text{intercept} - 23.76) \times 8.314 \text{ J mol}^{-1} \text{ K}^{-1}$ is the entropy of activation.

The free energy of activation (ΔG^*), was calculated from Eq. (2).

$$\Delta G^* = \Delta H^* - T\Delta S^* \quad (3)$$

The enthalpy, entropy, and free energy of activation associated with the inactivation process were determined by the linear Eyring plots for k_{inact} obtained in the presence of 1, 2 and 3 M NaCl.

2.9. Solvent kinetic isotope effects

The solvent kinetic isotope effects (SKIEs) on Nep activity were measured in 50 mM Tris–HCl pD 8.0 in the presence of 1, 2 or 3 M NaCl. The pD of deuterium oxide solution was calculated from pH meter readings according to the relationship $\text{pD} = \text{pH}(\text{meter reading}) + 0.4$ [28].

2.10. Circular dichroism

Far-UV circular dichroism (CD) spectra were recorded on a Jasco 136 J-810 spectropolarimeter (Jasco International Co.). CD measurements were carried out in a 1 mm quartz cuvette using the wavelength range of 202–260 nm. The protein concentration was set to 3.5 μM in 50 mM Tris–HCl (pH 8.0) with 1, 2 or 3 M NaCl. All samples were centrifuged at $10,000\times g$ for 10 min prior to analysis. Data collection parameters were set to scan rate of 50 nm/min, response time of 4 s, accumulation of 10, and delay time for spectrum collection of 60 s. Baseline subtraction, smoothing and data normalization were carried out using the graphical software ORIGIN (<http://www.originlab.com/>). CD data are shown as mean residue ellipticity units ($\text{deg cm}^2 \text{ dmol}^{-1} \text{ residue}^{-1}$).

2.11. Dynamic light scattering

DLS measurements were performed on a Dynapro Molecular Sizing instrument at 20 °C. The samples were previously centrifuged for 20 min at $20,000\times g$. In all conditions, samples were illuminated with a laser of 1 μm (diameter) and the intensity fluctuations from the scattered light were measured in a 1 cm path length quartz cell. The data were collected with intervals of 10 s with at least 100 acquisitions. The diffusion coefficient (D_T) was determined from the decay rate distribution of intensity correlation profiles and used to calculate the hydrodynamic radius (R_h) of the protein via Stokes–Einstein equation ($D_T = k_b T (6\pi\eta R_h)^{-1}$, where T is the temperature in Kelvin, k_b is the Boltzmann's constant and η is the solvent viscosity). Analysis was performed using the software Dynamics V6.3.40.

2.12. Small angle X-ray scattering

Small Angle X-ray Scattering (SAXS) data were collected at the D02A/SAXS2 beamline (Brazilian Synchrotron Light Laboratory, Campinas, Brazil). The radiation wavelength was set to 1.48 Å and a 165 mm MarCCD detector was used to record the scattering patterns. The sample-to-detector distance was set to 1534.5 mm to give a scattering vector-range from 0.18 to 2.1 nm^{-1} . Protein samples were prepared in 50 mM Tris–HCl (pH 8.0) with 1, 2 or 3 M NaCl. Prior to X-ray exposure, the samples were centrifuged at $20,000\times g$ for 10 min and then filtered to remove any existing aggregates. Buffer baselines were collected under identical conditions before and after sample data collection to guarantee accurate solvent correction. Frames with exposure time of 600 s were recorded to avoid radiation-induced protein damage. Background scattering was subtracted from the protein scattering pattern, which was then

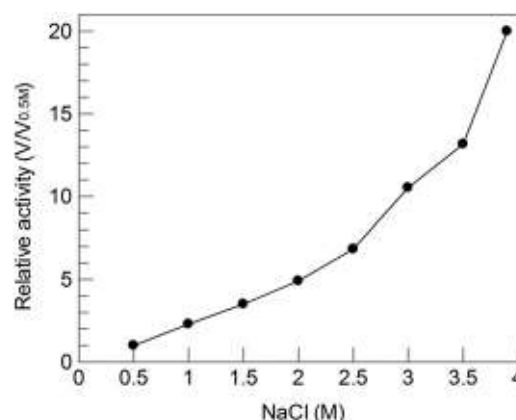


Fig. 1. Effect of NaCl concentration on Nep hydrolytic activity. Relative activities were determined by measuring the initial velocity of Suc-AAPF-MCA hydrolysis in the presence of NaCl at the concentration range from 0.5 to 4 M. Relative activities were calculated assuming the hydrolysis at 0.5 M of NaCl as 1 ($V/V_{0.5}$).

normalized and corrected. Experimental data fitting and evaluation of the pair-distance distribution function $p(r)$ were performed using the program GNOM [29]. The low-resolution envelope of Nep was determined using *ab initio* modeling as implemented in the program DAMMIN [30]. An averaged model was generated from several runs using the package DAMAVER [31]. The *in silico* models of both catalytic and C-terminal domains were modeled against the SAXS data using a combined rigid body and *ab initio* modeling approach, as implemented in the program BUNCH [32].

2.13. Homology molecular modeling

The atomic coordinates of Ak1 protease from *Bacillus* sp. (PDBID: 1DBI [33]) and collagen-binding domain from *Clostridium histolyticum* collagenase (PDBID: 1NQJ [34],) were used as templates for generating structural models of Nep from *N. magadii* by restraint-based modeling as implemented in the program MODELLER [35]. To guarantee sufficient conformational sampling, an ensemble of 50 models was built, from which the best final model was selected based on evaluation of the stereochemistry, the objective function from MODELLER (DOPE score) and by visual inspection. Those models were then minimized using the steepest descent minimization algorithm as implemented in the UCSF chimera software [36]. Incomplete site chains were replaced using Dunbrack rotamer library [37].

3. Results and discussion

3.1. Salt effect on Nep catalytic activity

The catalytic behavior of Nep using azocasein as substrate has been previously described and evidences the halophilic character of this subtilase [25]. To further examine this issue, hydrolysis velocity of the fluorogenic substrate Suc-Ala-Ala-Pro-Phe-MCA. Nep was inactive in the absence of salt, therefore, the relative activities were determined considering the value obtained at 0.5 M NaCl as 1. As shown in Fig. 1, the increase in Nep activity displayed a nonlinear concave-up dependence with salt concentration resulting in a 20-fold activation in 4.0 M NaCl. The same activation pattern was observed with the halophilic bacterial subtilase from *Halobacillus* sp. (SR5-3) that was reported to be active even in the absence of salt [18]. It is reported that some subtilases from prokaryotes bind calcium ions at specific binding sites and it seems to play a role in the enzyme stability and activity [33]. In order to address this issue,

Table 1

Salt effect on Nep kinetic parameters for hydrolysis of Suc-AAPF-MCA at 37 °C.

NaCl (M)	Tris 50 mM pH 8.0 (H ₂ O)			Tris 50 mM pD 8.0 (D ₂ O)			SKIE	
	k_{cat} (s ⁻¹)	K_{M} (μM)	$k_{\text{cat}}/K_{\text{M}}$ (mM s) ⁻¹	k_{cat} (s ⁻¹)	K_{M} (μM)	$k_{\text{cat}}/K_{\text{M}}$ (mM s) ⁻¹	$k_{\text{cat}}(\text{H}_2\text{O})/k_{\text{cat}}(\text{D}_2\text{O})$	$k_{\text{cat}}/K_{\text{M}}(\text{H}_2\text{O})/k_{\text{cat}}/K_{\text{M}}(\text{D}_2\text{O})$
1	2.7 ± 0.1	140 ± 9	19.3	0.6 ± 0.1	123 ± 13	5.0	4.5	3.9
2	5.3 ± 0.2	115 ± 10	46.1	1.1 ± 0.1	117 ± 9	9.4	4.8	4.9
3	6.3 ± 0.2	80 ± 5	78.7	1.5 ± 0.1	114 ± 6	12.7	4.3	6.5

Nep activity was tested in the presence of EDTA and calcium ions. Our results indicate that Nep enzymatic activity is not affected neither by 10 mM EDTA nor by different concentrations of calcium ions up to 300 mM (results not shown).

The pH dependence of Nep peptidase activity in the presence of 3 M NaCl was determined over the pH range of 6.3–10.5 (Supplementary Fig. S1). Maximum catalytic activity occurred above pH 8.0 with a sigmoid pH-rate profile characteristic of bacterial subtilases [38]. The obtained pK_{e} value ($pK_{\text{e}} = 6.8 \pm 0.3$) is related to catalytic histidine residue and it was similar to those values determined for SR5-3 bacterial subtilase ($pK_{\text{e}} = 7.2 \pm 0.2$) [18] and Carlsberg mesophilic subtilisin ($pK_{\text{e}} = 7.0$) [38].

The activation of Nep by NaCl was also investigated by the evaluation of the kinetic parameters (k_{cat} , K_{M} and $k_{\text{cat}}/K_{\text{M}}$) of the hydrolysis of the peptide Suc-AAPF-MCA in presence of 1, 2 and 3 M NaCl. As shown in Table 1, salt activation resulted from both increase in k_{cat} and K_{M} reduction as salt concentration increase from 1 to 3 M NaCl.

Solvent kinetic isotope effects (SKIEs) in Nep catalytic activity were analyzed to establish the presence of proton bridges in the rate-determining transitions state(s) of its general acid-base-catalyzed reaction [39–42]. Likewise to serine-peptidases, the peptide hydrolysis in deuterium oxide (D₂O) occurred slower with a significant decrease of $k_{\text{cat}}/K_{\text{M}}$ and k_{cat} parameters in buffers containing 1–3 M NaCl and resulted in SKIE values [$k(\text{H}_2\text{O})/k(\text{D}_2\text{O})$] varying from 4.3 to 4.8 for k_{cat} and 3.9 to 6.5 for $k_{\text{cat}}/K_{\text{M}}$ (Table 1). These results support the notion that a general acid-base reaction is the rate-limiting step for Nep catalytic activity and that it is not affected by salt activation.

It should be emphasized that short time incubations of the enzyme in a low-saline (1 M NaCl) or high-saline (3 M NaCl) solutions resulted in similar velocities of hydrolysis; however, longer incubations in solutions with low or moderated salinities decreased Nep activity. Thus, to clarify this observation, the salt effect on both Nep activity and stability were examined in the following experiments.

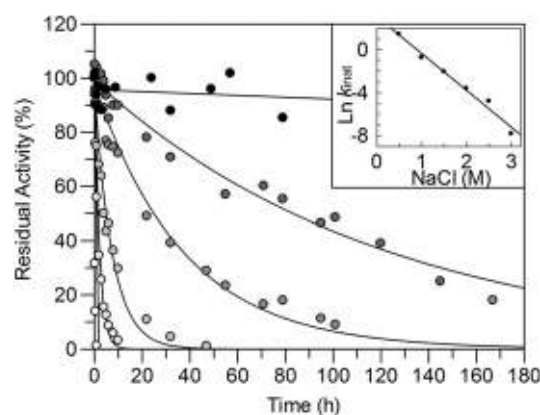


Fig. 2. Salt effect on Nep stability at 37 °C. Activities were measured in reconstituted 3 M NaCl-containing buffer after incubation in 50 mM Tris–HCl with 0.5 M NaCl (○), 1 M NaCl (●), 1.5 M NaCl (●), 2 M NaCl (●), 2.5 M NaCl (●) and 3 M NaCl (●). Inset: Dependence of salt concentration of $\ln k_{\text{inat}}$.

3.2. Salt effect on Nep stability

Nep stability (i.e. the capacity of an enzyme molecule to resist unfolding in the absence of substrate) was evaluated in different salt concentrations ranging from 0 to 4 M NaCl at 37 °C. Activities were screened against time and the results are shown in Fig. 2. Incubation in the absence of salt resulted in complete loss of activity even at the shortest interval analyzed ($t = 30$ s). On the other hand, inactivation rate constants could not be obtained above 3 M NaCl since any loss of activity was observed after 1 month incubation under the same conditions (data not shown). Inactivation was shown to follow first-order kinetics in the 0.5–3.0 M NaCl range, where increase in salt concentration decreased inactivation rate constants, k_{inat} , from 4.2 ± 0.2 h⁻¹ at 0.5 M to 4.10^{-4} h⁻¹ at 3.0 M NaCl and, consequently, increase of the half-life from 10 min to 2 months at 3 M NaCl (Supplementary Table S1). The protective effect of salt against Nep unfolding is highlighted by the linearity found in the plot of $\ln k_{\text{inat}}$ over salt concentration at 37 °C (Fig. 2, inset).

In order to check for the reversibility of the observed inactivation process, 0.5 and 1 M NaCl half-life samples were reconstituted in buffer containing 3 M NaCl and their activity screened for up to 48 h. In both cases, activity remained constant at ~50% of maximum (data not shown) indicating that Nep inactivation induced by decrease in salt concentration is an irreversible process. It should be pointed out that Nep, incubated in absence of salt for 1 min, remains inactive (i.e. do not recover activity) after reconstitution in 3 M NaCl buffer for 48 h.

The effect of temperature on Nep stability in a hypersaline environment (3 M NaCl) was determined over the temperature range from 37 to 65 °C (Fig. 3). The enzyme was found to be stable in the range of 4–37 °C for several days in presence of 3 M NaCl (results not shown). Data fitting to Eq. (1) indicates that thermal inactivation kinetics followed first order in all cases and, as expected, higher temperatures significantly increase inactivation rate constants (k_{inat}) and decrease the half-life ($t_{1/2}$) (Supplementary Table S1). Similar experiment conducted at low (1 M NaCl) and

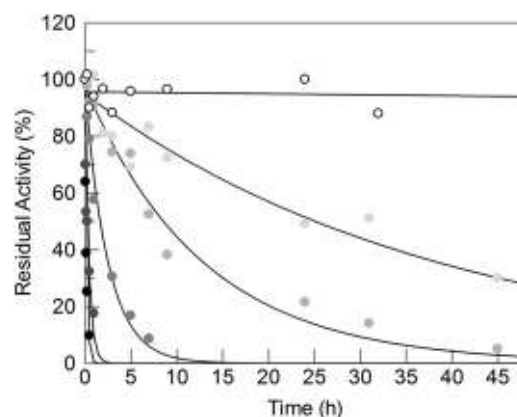


Fig. 3. Nep thermal stability in the presence of 3 M NaCl. Activities were measured at 37 °C in 50 mM Tris–HCl (pH 8.0) with 3 M NaCl after incubation in the same buffer at 37 (○) 45 (●), 50 (●), 55 (●), 60 (●) and 65 °C (●).

Table 2
Salt effect on thermodynamic parameters for Nep thermal stability (k_{inat}) and activity on Suc-AAPF-MCA (k_{cat}/K_M).

NaCl (M)	Stability			Activity		
	ΔH^* (kJ/mol)	ΔS^* (J/mol K)	ΔG^* (kJ/mol)	ΔH^* (kJ/mol)	ΔS^* (J/mol K)	ΔG^* (kJ/mol)
1	229 ± 14	447 ± 32	84	15 ± 2	−131 ± 11	55
2	260 ± 13	540 ± 30	93	25 ± 2	−90 ± 7	53
3	316 ± 15	691 ± 41	102	32 ± 1	−63 ± 4	51

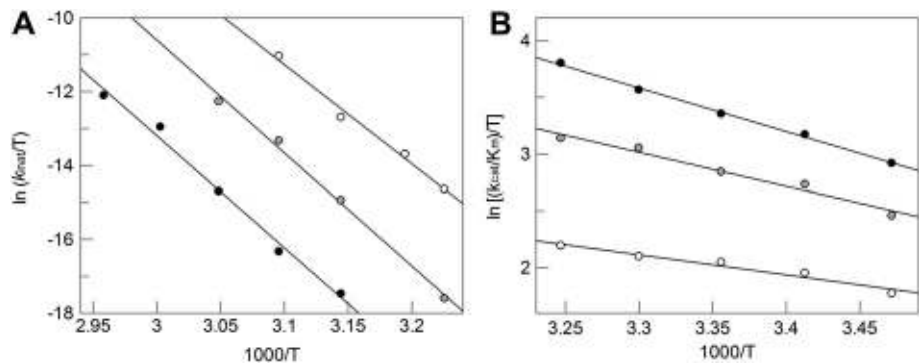


Fig. 4. Eyring plots for Nep stability (A) and catalysis (B). The apparent first-order rate constants for thermal inactivation of Nep (k_{inat}) in the presence of 1 (○), 2 (◐) and 3 M (●) NaCl.

moderate (2 M NaCl) salinities enabled a detailed thermodynamic characterization of NaCl effect on Nep stability. The entropy (ΔS_{inat}), enthalpy (ΔH_{inat}), and Gibbs free energy of activation (ΔG_{inat}) associated with the inactivation process (Table 2) were determined by the linear Eyring plots for k_{inat} obtained in the presence of 1, 2 and 3 M NaCl (Fig. 4A).

The free-energy term is a reliable indicator of enzyme stability since it includes the contributions from both enthalpic and entropic terms [43]. In this sense, the smaller standard-state free-energy change observed in low salinity is an indicative of less stable enzyme and the protective effect of salt can be calculated by the linear dependence of ΔG_{inat} on the salt concentration, i.e., the $\Delta(\Delta G_{\text{inat}})/\Delta[\text{NaCl}]$ that is equal to 9 ± 2 kJ/mol/M (Supplementary Fig. S2). Conversely, higher salinities were associated with higher enthalpic and entropic terms, with $\Delta(\Delta H_{\text{inat}})/\Delta[\text{NaCl}]$ and $\Delta(\Delta S_{\text{inat}})/\Delta[\text{NaCl}]$ values equal to 44 ± 7 kJ/mol K/M and 122 ± 16 J/mol K/M, respectively. The large and positive $\Delta(\Delta H_{\text{inat}})/\Delta[\text{NaCl}]$ indicates that greater amounts of energy are required for the

denaturation process to occur at higher salinities, whereas the positive salt effect on the entropic term is indicative of disorder increase, or randomness, of the system (protein–solvent) upon denaturation.

3.3. Salt effect on temperature dependence of Nep activity

The hydrolysis of Suc-AAPF-MCA by Nep in the presence of 1, 2 and 3 M NaCl over the temperature range of 15–30 °C was analyzed and from the linear Eyring plot, the entropy (ΔS^*), enthalpy (ΔH^*) and Gibbs free energy of activation (ΔG^*) associated with the rate-limiting step of Nep hydrolysis was calculated (Table 2 and Supplementary Fig. S2). It is outstanding that the decrease in salt concentration from 3 to 1 M resulted in more negative ΔS^* . While solvent effects certainly interfere with the observed entropic change, a negative entropic contribution is expected to result from the freezing in translational and rotational motion that occurs when the reactants go from the ground state (E + S) to the enzyme–substrate

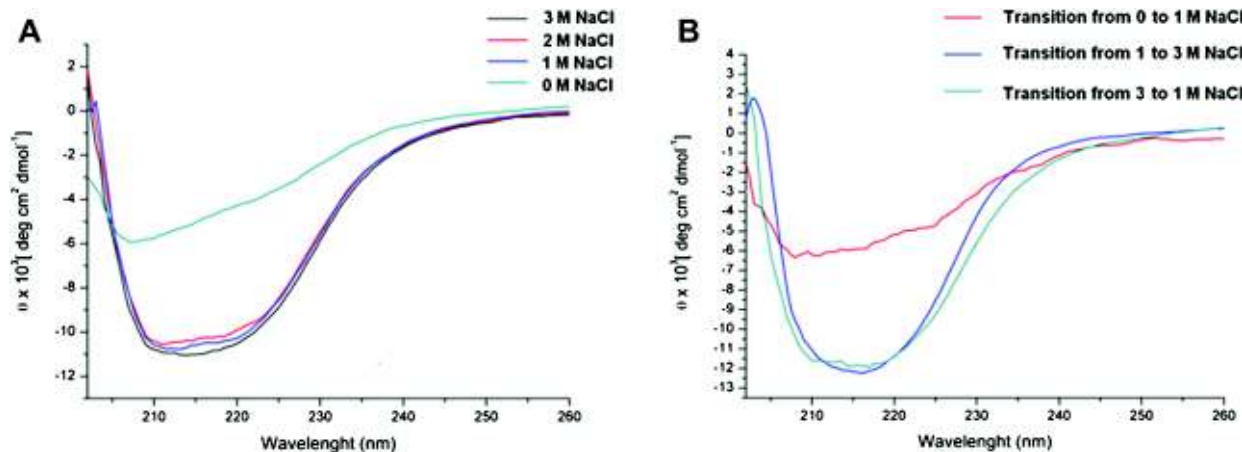


Fig. 5. Circular dichroism experiments. (A) Residual molar ellipticities of Nep at different salt concentrations were measured in the wavelength range 202–260 nm. (B) CD spectra of Nep in transitions from low-saline to high-saline environments.

Table 3
Hydrodynamic behavior of Nep at different salt concentrations.

NaCl (M)	R_h (nm) (from DLS data) ^a	R_g (nm) (from SAXS data) ^a	Polydispersity (%)
1	2.92 ± 0.31	2.71 ± 0.03	25
2	3.41 ± 0.25	2.90 ± 0.02	27
3	3.90 ± 0.39	3.03 ± 0.05	20

^a R_h – Hydrodynamic radius; R_g – Gyration radius.

complex (ES). In this sense, the salt effect on entropy term ($\Delta(\Delta S_{cat})/\Delta_{[NaCl]} = 34 \pm 4 \text{ J/mol K/M}$) may indicate that at 3 M NaCl the enzyme is more flexible than in 1 M. The steady-state analysis revealed that salt affects all steps of the substrate hydrolysis through enhancing the ES complex concentration. High salt concentration also promotes a large increase in the k_{cat} value (Table 1), suggesting that the diffusion of both substrate and catalytic water is increased at high salt concentration. The gain of order to reach the transition state at 1 M NaCl is greater than at 3 M, i.e., a larger Nep reorganization is needed at 1 M than at 3 M NaCl. These data suggest that the loss of

activity observed at 1 M NaCl can be related to a more rigid conformation of the enzyme.

3.4. Salt effect on Nep secondary structure

Far-UV CD spectra of Nep in different salt concentrations indicate that the enzyme remains folded in 1, 2 and 3 M NaCl without significant changes in secondary structure contents (Fig. 5A). The transfer from a low-saline (1 M NaCl) to a high-saline environment (3 M NaCl) or vice versa did not result in CD spectral changes (Fig. 5B); however, enzymatic activity is suppressed when the salinity is decreased to 1 M (NaCl). In the absence of salt, the enzyme displayed a typical CD spectrum of coil structure (Fig. 5B) and it is characterized as an irreversible process, since adding 3 M NaCl in a salt-free Nep sample, the native spectrum is not recovered (Fig. 5B). These results suggest that the changes in the enzymatic behavior and protein stability can be related to the tertiary structure conformation. Thus, in order to elucidate the tertiary structure arrangement of Nep in different salt concentrations, DLS and SAXS experiments were performed.

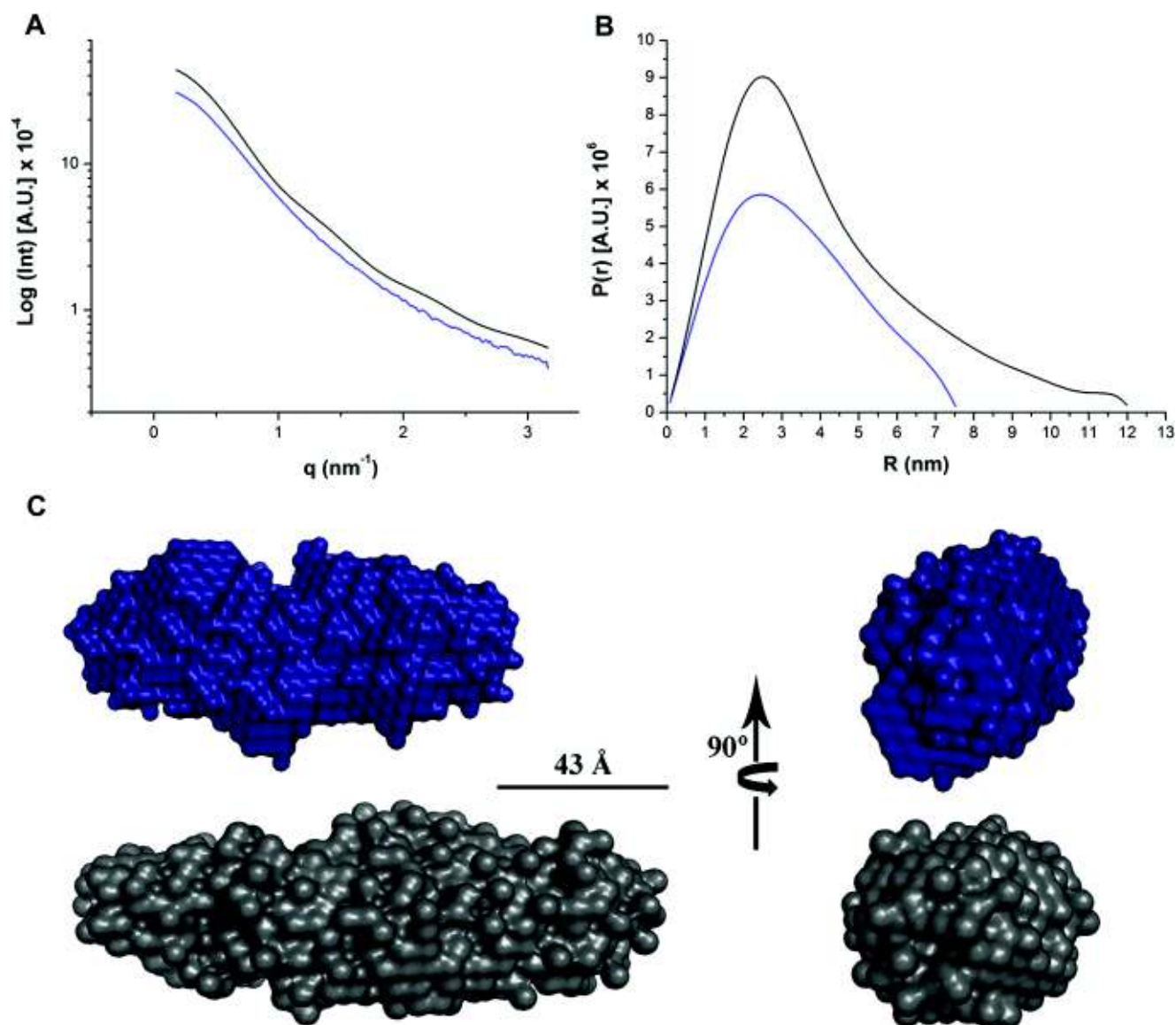


Fig. 6. SAXS data. (A) Experimental scattering curves and (B) pair-distance distribution function $p(r)$ of Nep at 1 M (blue) and 3 M NaCl (gray). (C) SAXS envelopes of Nep at 1 M NaCl (blue) and 3 M NaCl (gray). (For interpretation of the references to colour in this figure legend, the reader is referred to the web version of this article.)

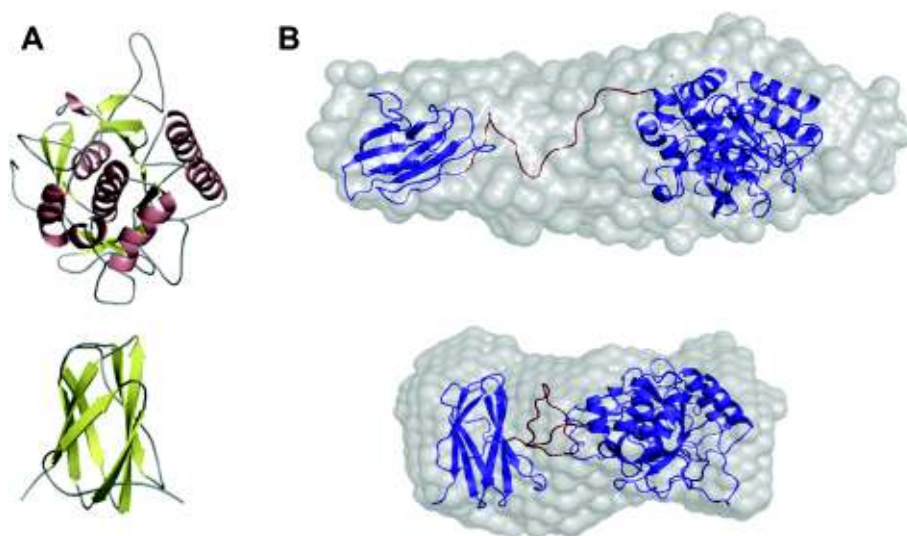


Fig. 7. Fitting of the atomic coordinates into SAXS envelope. (A) Models of N- (upper) and C-terminal (lower) domains of Nep. (B) Superposition of Nep structure on the SAXS envelope obtained at 1 M and 3 M NaCl.

3.5. Salt effect on Nep hydrodynamic behavior

The size distribution profile of Nep in the presence of different salt concentrations (0, 1, 2 or 3 M NaCl) was investigated by DLS indicating that Nep exists as individually dispersed molecules in environments with NaCl concentration above 1 M (Table 3). However, in a salt-free solution, Nep forms soluble aggregates, which are not untied by incubation with 3 M NaCl.

Interestingly, the hydrodynamic radius (R_h) of Nep shifted to smaller size ranges with the reduction of salt concentration (Table 3). At 3 M NaCl, the enzyme displays an R_h of 3.9 nm, whereas at 1 M NaCl, its R_h is 2.9 nm. This molecular shortening, in conjunction with the observed NaCl effects on both activity and stability, supports the notion that a conformational transition, triggered by the decrease in the salt concentration, affects the biological function of Nep.

3.6. Low-resolution structure and salt-induced conformational states

The molecular conformation of Nep in the presence of 1, 2 or 3 M NaCl was also analyzed by SAXS. From the scattering and pair-distance distribution curves (Fig. 6A–B), it is possible to observe the maximum molecular dimension (D_{max}) differing under different salt conditions. The gyration radii obtained from SAXS data corroborate with the hydrodynamic radii calculated from DLS data (Table 3), taking into account that the hydrated protein radius (DLS) is typically larger than the gyration radius (SAXS).

Low-resolution structures of Nep at 1 and 3 M NaCl, generated by *ab initio* calculations, give a clear view that the inter-domain structural arrangement is driven by environmental salinity. Superposition of these SAXS envelopes showed a molecular shortening of around 40 Å when the salt concentration is changed from 3 to 1 M NaCl (Fig. 6C).

In order to correlate low-resolution models with atomic coordinates, molecular modeling methods were employed to obtain the structures of both catalytic core and C-terminal domain of Nep. The N-terminus (1–286) is an α/β catalytic domain found in members of the peptidase S8 (subtilisin and kexin) family and the C-terminal domain (311–416) comprises two β -sheet motifs with 4 and 5 β -strains each (Fig. 7A). Fitting of both domains into the SAXS

envelopes obtained at 1 and 3 M NaCl suggests an inter-domain dissociation in a salt-dependent manner (Fig. 7B) and this structural state is correlated with optimal stability and activity. These domains are linked by a 37-residue long loop rich in glutamate residues, which in its extended form, can reach a length of 46 Å according to the dimensions observed in the SAXS data and structural model. It is proposed that the neutralization of negative charges on the surface of halophilic proteins by the salt counterions plays an important role in the maintaining of the native structure [19,44,45]. Based on this fact, we suggest that the electrostatic neutralization of the highly negatively charged linker can affect overall Nep structure as indicated by SAXS and DLS data. The fact of both R_h and R_g diminish with the decrease of salt concentration support the hypothesis that environmental counter-ions can dictate the linker orientation and consequently the three-dimensional arrangement of domains. Moreover, the lack of catalytic activity in absence of salt as described herein and previously [24,46] can also be addressed to the closure of structure, which due to the proximity of C-terminal domain to active-site pocket may result in a steric hindrance (Fig. 7B).

4. Conclusions

Nep hydrodynamic behavior was investigated by DLS and SAXS suggesting a molecular strategy that deal with large structural rearrangements caused by variations in environmental salinity. Extensive biochemical characterization showed the importance of high environmental salinity for catalysis and stability. Increase in salt concentration enhances Nep half-life at 37 °C from a few minutes at 0.5 M NaCl to at least two months above 3 M. In the absence of salt, CD data showed that the enzyme undergoes denaturation followed by the formation of non-active soluble aggregates. Despite no changes in the secondary structure contents were observed at NaCl range from 1 to 3 M, both DLS and SAXS measurements indicate that salinity do affect tertiary structural arrangement with its full-active form at 3 M NaCl encompassing an elongated conformation without inter-domain interactions. Those tertiary structure changes triggered by environmental salinity are also corroborated by thermodynamic analysis, where the more negative value of the entropic term indicates the need of large enzyme reorganization for catalysis in moderate salt environments.

These data correlate kinetic and structural behavior of Nep depicting a comprehensive description of the dynamics involved in functioning of halolysins under different salinities.

Acknowledgments

This work was supported by the Brazilian research agencies Fundação de Amparo à Pesquisa do Estado de São Paulo (FAPESP), Conselho Nacional de Desenvolvimento Científico e Tecnológico (CNPq), Coordenação de Aperfeiçoamento de Pessoal de Nível Superior (CAPES) and the Argentinian research agency Ministerio de Ciencia, Tecnología e Innovación Productiva (MINCYT) (Cooperative Research Project MINCYT-CAPES, BR09/04). D.M. Ruiz is a PhD student supported by the Consejo Nacional de Investigaciones Científicas y Técnicas (CONICET), Argentina.

Appendix. Supplementary data

Supplementary data related to this article can be found online at doi:10.1016/j.biochi.2011.11.011.

References

- [1] R.J. Siezen, J.A.M. Leunissen, Subtilases: the superfamily of subtilisin-like serine proteases, *Protein Sci.* 6 (1997) 501–523.
- [2] M.B. Rao, A.M. Tanksale, M.S. Ghatge, V.V. Deshpande, Molecular and biotechnological aspects of microbial proteases, *Microbiol. Mol. Biol. Rev.* 62 (1998) 597–635.
- [3] R. Gupta, Q.K. Beg, P. Lorenz, Bacterial alkaline proteases: molecular approaches and industrial applications, *Appl. Microbiol. Biotechnol.* 59 (2002) 15–32.
- [4] M.D. Ballinger, J. Tom, J.A. Wells, Designing subtilisin BPN⁺ to cleave substrates containing dibasic residues, *Biochemistry* 34 (1995) 13312–13319.
- [5] P.R. Bonneau, T.P. Graycar, D.A. Estell, J.B. Jones, Alteration of the specificity of subtilisin BPN⁺ by site-directed mutagenesis in its S₁ and S₁′, *J. Am. Chem. Soc.* 113 (1991) 1026–1030.
- [6] G. DeSantis, P. Berglund, M.R. Stabile, M. Gold, J.B. Jones, Site-directed mutagenesis combined with chemical modification as a strategy for altering the specificity of the S₁ and S₁′ pockets of subtilisin *Bacillus lentus*, *Biochemistry* 37 (1998) 5968–5973.
- [7] M. Rheinacker, J. Eder, P.S. Pandey, A.R. Fersht, Variants of subtilisin BPN⁺ with altered specificity profiles, *Biochemistry* 33 (1994) 221–225.
- [8] B. Ruan, V. London, K.E. Fisher, D.T. Gallagher, P.N. Bryan, Engineering substrate preference in subtilisin: structural and kinetic analysis of a specificity mutant, *Biochemistry* 47 (2008) 6628–6636.
- [9] S. Davail, G. Feller, E. Narinx, C. Gerday, Cold adaptation of proteins. Purification, characterization, and sequence of the heat-labile subtilisin from the antarctic psychrophile *Bacillus TA41*, *J. Biol. Chem.* 269 (1994) 17448–17453.
- [10] Y. Kannan, Y. Koga, Y. Inoue, M. Haruki, M. Takagi, T. Imanaka, M. Morikawa, S. Kanaya, Active subtilisin-like protease from a hyperthermophilic archaeon in a form with a putative prosequence, *Appl. Environ. Microbiol.* 67 (2001) 2445–2452.
- [11] T. Tanaka, H. Matsuzawa, S. Kojima, I. Kumagai, K. Miura, T. Ohta, P1 specificity of aqualysin I (a subtilisin-type serine protease) from *Thermus aquaticus* YT-1, using P1-substituted derivatives of Streptomyces subtilisin inhibitor, *Biosci. Biotechnol. Biochem.* 62 (1998) 2035–2038.
- [12] Y. Yamagata, K. Isshiki, E. Ichishima, Subtilisin Sendai from alkalophilic *Bacillus* sp.: molecular and enzymatic properties of the enzyme and molecular cloning and characterization of the gene, *aprs*, *Enzym. Microb. Technol.* 17 (1995) 653–663.
- [13] E. Mellado, C. Sanchez-Porro, A. Ventosa, Proteases produced by halophilic bacteria and archaea, in: J.L. Barredo (Ed.), *Microbial Enzymes and Biotransformations*, Humana Press Inc., 2005, pp. 181–190.
- [14] R.E. de Castro, J.A. Maupin-Furlow, M.I. Gimenez, M.K. Herrera-Seitz, J.J. Sanchez, Haloarchaeal proteases and proteolytic systems, *FEMS Microbiol.* 30 (2006) 17–35.
- [15] W. Shi, X.F. Tang, Y. Huang, F. Gan, B. Tang, P. Shen, An extracellular halophilic protease SptA from a halophilic archaeon *Natrinema* sp. J17: gene cloning, expression and characterization, *Extremophiles* 10 (2006) 599–606.
- [16] M. Vidyasagar, S. Prakash, C. Litchfield, K. Sreeramulu, Purification and characterization of a thermostable, haloalkaliphilic extracellular serine protease from the extreme halophilic archaeon *Haloquadratum walsbyi* strain TSS101, *Archaea* 2 (2006) 51–57.
- [17] H.R. Karbalaee-Heidari, A.A. Ziaee, M.A. Amoozegar, Purification and biochemical characterization of a protease secreted by the *Salinivibrio* sp. strain AF-2004 and its behavior in organic solvents, *Extremophiles* 11 (2007) 237–243.
- [18] D.N. Okamoto, M.Y. Kondo, K. Hiraga, M.A. Juliano, L. Juliano, I.E. Gouvea, K. Oda, Salt effect on substrate specificity of a subtilisin-like halophilic protease, *Protein Pept. Lett.* 17 (2010) 796–802.
- [19] D.N. Okamoto, M.Y. Kondo, J.A. Santos, S. Nakajima, K. Hiraga, K. Oda, M.A. Juliano, L. Juliano, I.E. Gouvea, Kinetic analysis of salting activation of a subtilisin-like halophilic protease, *Biochim. Biophys. Acta* 1794 (2009) 367–373.
- [20] D. Madern, C. Ebel, G. Zaccari, Halophilic adaptation of enzymes, *Extremophiles* 4 (2000) 91–98.
- [21] M. Mevarech, F. Frolow, L.M. Gloss, Halophilic enzymes: proteins with a grain of salt, *Biophys. Chem.* 86 (2000) 155–164.
- [22] M. Kamekura, Y. Seno, M.L. Holmes, M.L. Dyall-Smith, Molecular cloning and sequencing of the gene for a halophilic alkaline serine protease (halolysin) from an unidentified halophilic archaea strain (172P1) and expression of the gene in *Haloferax volcanii*, *J. Bacteriol.* 174 (1992) 736–742.
- [23] M. Kamekura, Y. Seno, M. Dyall-Smith, Halolysin R4, a serine proteinase from the halophilic archaeon *Haloferax mediterranei*; gene cloning, expression and structural studies, *Biochim. Biophys. Acta* 1294 (1996) 159–167.
- [24] R.E. de Castro, D.M. Ruiz, M.I. Gimenez, M.X. Silveyra, R.A. Paggi, J.A. Maupin-Furlon, Gene cloning and heterologous synthesis of a haloalkaliphilic extracellular protease of *Natrialba magadii* (Nep), *Extremophiles* 12 (2008) 677–687.
- [25] M.I. Gimenez, C.A. Studdert, J.J. Sanchez, R.E. de Castro, Extracellular protease of *Natrialba magadii*: purification and biochemical characterization, *Extremophiles* 4 (2000) 181–188.
- [26] L. Polgar, Oligopeptidase B: a new type of serine peptidase with a unique substrate-dependent temperature sensitivity, *Biochemistry* 38 (1999) 15548–15555.
- [27] A. Cornish-Bowden, Enzyme kinetics from a metabolic perspective, *Biochem. Soc. Trans.* 27 (1999) 281–284.
- [28] P.K. Glasoe, F.A. Long, Use of glass electrodes to measure acidities in deuterium oxide, *J. Phys. Chem.* 64 (1960) 188–190.
- [29] D.I. Svergun, Determination of the regularization parameter in indirect-transform methods using perceptual criteria, *J. Appl. Crystallogr.* 25 (1992) 495–503.
- [30] D.I. Svergun, Restoring low resolution structure of biological macromolecules from solution scattering using simulated annealing, *Biophys. J.* 76 (1999) 2879–2886.
- [31] V.V. Volkov, D.I. Svergun, Uniqueness of ab initio shape determination in small-angle scattering, *J. Appl. Cryst.* 36 (2003) 860–864.
- [32] M.V. Petoukhov, D.I. Svergun, Global rigid body modelling of macromolecular complexes against small-angle scattering data, *Biophys. J.* 89 (2005) 1237–1250.
- [33] C.A. Smith, H.S. Toogood, H.M. Baker, R.M. Daniel, E.N. Baker, Calcium-mediated thermostability in the subtilisin superfamily: the crystal structure of *Bacillus* Ak.1 protease at 1.8 Å resolution, *J. Mol. Biol.* 294 (1999) 1027–1040.
- [34] J.J. Wilson, O. Matsushita, A. Okabe, J. Sakon, A bacterial collagen-binding domain with novel calcium-binding motif controls domain orientation, *EMBO J.* 22 (2003) 1743–1752.
- [35] A. Sali, T.L. Blundell, Comparative protein modelling by satisfaction of spatial restraints, *J. Mol. Biol.* 234 (1993) 779–815.
- [36] E.F. Pettersen, T.D. Goddard, C.C. Huang, G.S. Couch, D.M. Greenblatt, E.C. Meng, T.E. Ferrin, UCSF Chimera—a visualization system for exploratory research and analysis, *J. Comput. Chem.* 25 (2004) 1605–1612.
- [37] R.L. Dunbrack Jr., Rotamer libraries in the 21st century, *Curr. Opin. Struct. Biol.* 12 (2002) 431–440.
- [38] M. Philipp, I.H. Tsai, M.L. Bender, Comparison of the kinetic specificity of subtilisin and thiolsubtilisin toward n-alkyl p-nitrophenyl esters, *Biochemistry* 18 (1979) 3769–3773.
- [39] K.B. Schowen, H.H. Limbach, G.S. Denisov, R.L. Schowen, Hydrogen bonds and proton transfer in general-catalytic transition-state stabilization in enzyme catalysis, *Biochim. Biophys. Acta* 1458 (2000) 43–62.
- [40] K.B. Schowen, R.L. Schowen, Solvent isotope effects of enzyme systems, *Methods Enzymol.* 87 (1982) 551–606.
- [41] E.J. Enyedy, I.M. Kovach, Proton inventory studies of alpha-thrombin-catalyzed reactions of substrates with selected P and P′ sites, *J. Am. Chem. Soc.* 126 (2004) 6017–6024.
- [42] M.Y. Kondo, D.N. Okamoto, J.A. Santos, M.A. Juliano, K. Oda, B. Pillai, M.N. James, L. Juliano, I.E. Gouvea, Studies on the catalytic mechanism of a glutamic peptidase, *J. Biol. Chem.* 285 (2010) 21437–21445.
- [43] A.G. Marangoni, *Enzyme Kinetics: A Modern Approach*, first ed. John Wiley & Sons, Inc., 2003.
- [44] O. Dym, M. Mevarech, J.L. Sussman, Structural features that stabilize halophilic malate dehydrogenase from an archaeobacterium, *Science* 267 (1995) 1344–1346.
- [45] F. Frolow, M. Harel, J.L. Sussman, M. Mevarech, M. Shoham, Insights into protein adaptation to a saturated salt environment from the crystal structure of a halophilic 2Fe-2S ferredoxin, *Nat. Struct. Biol.* 3 (1996) 452–458.
- [46] D.M. Ruiz, R.E. de Castro, Effect of organic solvents on the activity and stability of an extracellular protease secreted by the haloalkaliphilic archaeon *Natrialba magadii*, *J. Ind. Microbiol. Biotechnol.* 34 (2007) 111–115.